Volume 18, No 3 | International Journal of Radiation Research, July 2020

Tumor shrinkage evaluation based interfractional cone beam computed tomography for limited disease small-cell lung cancer and relevant impact on dosimetry

H. Wang[1], H. Chen[2], Y. Shao[2], J.M. Wang[2], J.D. Guo[2], X.W. Cai[2], X.I. Fu[2], Z.Y. Xu[2]*

[1]Key Laboratory of Nuclear Physics and Ion-beam Application(MOE), Fudan University, Shanghai, China
[2]Radiation Oncology Department, Shanghai Chest Hospital, Shanghai Jiao Tong University, Shanghai, China

► ***Original article***

Corresponding authors:
Prof. Zhiyong Xu,
E-mail:
xzyong12vip@sina.com

Revised: April 2019
Accepted: December 2019

Int. J. Radiat. Res., July 2020; 18(3): 467-475

DOI: 10.18869/acadpub.ijrr.18.3.467

ABSTRACT

Background: The pattern of interfractional tumor changes during limited disease small-cell lung cancer (LD-SCLC) radiotherapy is not clear, The study was to evaluate tumor changes based on interfractional CBCT images and it's impact on dosimetry. ***Material and Method:*** We analyzed tumor changes and it's dosimetry impact for 30 LD-SCLC patients who were treated with concurrent chemoradiotherapy(cCRT). CBCT images were acquired for each patient every five fractions before each treatment. The grass tumor volume (GTV) and total lung were adapted to create the GTV_n and total $lung_n$ based on $CBCT_n$. Dose was recalculated for every CBCT fraction. The impact on target dose coverage and lung sparing was also evaluated while relevant tissue's CT density correction was done on plan CT combined with tumor changes adapted by fraction's CBCT images. ***Results:*** Mean GTV volume of each CBCT fraction reduced，and mean GTV volume of 7th CBCT fraction shrank nearly 10% compared to 1st fraction. The centroid positions of left/right tumors moved towards the right/left direction gradually. Most left/right tumor borders had a trend of rightward/leftward shrinkage. Target dose coverage and lung tissue dose volume increased through fractions. CT image density correction slightly increased the target dose coverage and lung tissue dose volume. ***Conclusion:*** Tumor shrinkage was seen for LD-SCLC patients, it's related to the tumor's initial volume and location. It is appropriate that most LD-SCLC patients should be intervened at 21st radiotherapy fraction.

Keywords: *Tumor shrinkage; interfractional cone beam CT; dosimetry; limited disease (LD) small-cell lung cancer.*

INTRODUCTION

About 20% cases of lung cancer are small-cell lung cancer (SCLC). The most common staging system for SCLC is that by Veterans Administration Lung Study Group (VALG): limited disease (LD) and extensive disease (ED). This staging system is simple and easy to apply, and it's corresponding to treatment efficacy and prognosis. Currently, Tumor node metastasis (TNM) staging is also used by SCLC [1]. Less than 5% of SCLC patients are in the early stage, when tumor is only limited in pulmonary parenchyma. These patients can consider surgical treatment. LD-SCLC patients are mainly treated by concurrent or sequential chemoradiotherapy, and concurrent chemoradiotherapy (cCRT) is the prior choice. CCRT should be applied as early as possible, and should be combined with prophylactic cranial irradiation (PCI) which benefits survival significantly [2-6].

Higher radiotherapy dose is restricted due to the need to spare organs at risk (OARs), therefore it is necessary to provide individual treatment to patient to maximize therapeutic gain ratio. Cone beam CT(CBCT) can accurately

[DOI: 10.18869/acadpub.ijrr.18.3.467]

evaluate SCLC patients' tumor changes [7-8], and adaptive radiotherapy can be delivered timely while significantly shrunk tumor was observed, as a result, target dose can be increased while normal tissues were spared.

Currently, the pattern of tumor change during SCLC radiotherapy is not clear, so it is very important to observe the tumor during the treatment. The main reason for SCLC treatment failure is its short doubling time and therefore fast growth speed [9]; 8 different patterns of tumor expansion and invasion to the periphery may occur for SCLC[100]; tumor changes during the radiotherapy is an effect combining lung cancer cells doubling and the inactivation of cancer cells by radiation beams.

As SCLC doubling time is short and the number of cases is small, few papers reported the pattern of tumor changes, and it's still not clear that how to find the particular group who might mostly benefited from adaptive radiotherapy as well as the best intervention time. In this study, 30 LD-SCLC patients were recruited. automated planning was used to complete IMRT plans, and CBCT images were acquired for the patients before specific treatment fractions. The changes of tumor's volume, centroid position and boundary during the treatment were evaluated.

P Berkovic, *et al.* [11] reported the impact of tumor volume changes on target and OARs doses by plan CT images while relevant structures' CT densities were not corrected for nonsmall- cell lung cancer (NSCLC). One of the vital improvements in this study was that relevant structures' CT densities correction was made while tumor volumes were adapted by fractions' CBCT images for LD-SCLC, thus the dose calculation accuracy was closer to real delivery dose without reoptimization. At the same time, this study is a first attempt to clarify the most proper intervention time for LD-SCLC radiotherapy.

MATERIALS AND METHODS

Patients

Ethics committee approval was obtained from the Institutional Ethics Committee of Shanghai Chest Hospital for the study. Cases information: 30 LD-SCLC patients were recruited during March 2015 to December 2016. There were 24 male and 6 female patients, 12 left and 18 right lung cancer patients, 26 central and 4 peripheral lung cancer patients, 15 T2 stage, 12 T3 stage, 2 T4 stage patients. The initial intrapulmonary tumors volume range was 45.3~113.5 cm^3. All patients have signed the informed consent. Treatment methods: cCRT induced by chemotherapy while the radiotherapy doses were 60 Gy/30(23 cases), 55 Gy/22(5 cases) and 59.4 Gy/27(2 cases). Concurrent chemotherapy was performed in 1-4 days of etoposide plus platinum (EP) treatment.

Table 1. Clinical characteristics of 30 patients.

		%
Mean age, years		**62 (range 44–78)**
Gender		
male	24	80
female	6	20
Tumor location		
left	12	40
right	18	60
central	26	86.7
peripheral	4	13.3
TNM		
T2aN1M0	5	16.7
T2bN2M0	9	30
T2N3Mx	1	3.3
T3N2M0	6	20
T3N2M1	2	6.7
T3N3M0	4	13.3
T4N2M1	2	6.7
TxN2M0	1	3.3
GTV volume		45.3~113.5 cm^3

Simulation

The patients were positioned in supine position and fixed with negative pressure bags while both arms raised and crossed; patient's two hands held the positioning bed handles. CT scan started from cervical vertebra C3, to the lower edge of the liver including the entire lung; the thickness of CT scan was 3 mm. The images were transferred to Pinnacle 9.10 treatment planning system (Philips Medical Systems, USA).

Contour

Each patient's simulation CT images were

[DOI: 10.18869/acadpub.ijrr.18.3.467]

fused with 18F positron emission tomography / computed tomography (PET/CT); then a physician with more than 5 years clinical experience delineated the gross target volume (GTV). Based on imaging and clinical examination results, the physician defined the intrapulmonary tumor as well as high metabolic value mediastinal lymph nodes as the GTV on the CT images. Organs at risk included left lung, right lung, total lung (All lung minus intrapulmonary GTV), spinal cord and the heart. The planned target volume (PTV) was formed by expanding 5 mm from GTV while the margin was adjusted by the patient's actual respiratory mobility.

Planning

Treatment planning was completed by the automatic optimization module in Pinnacle 9.10 Planning System (Philips Medical Systems, USA). Synergy accelerator (Elekta Company, Sweden) was used for delivery which can provide 6 MV X-ray beam and 40 pairs leaves of MLC with 10 mm leaf thickness. 4-5 fields' static IMRT plans were used for treatment.

CBCT images

XVI System of the Synergy linear accelerator was used for CBCT images acquisition. CBCT images were acquired when the patients' setups were completed before their first radiotherapy. Auto registration combined with manual registration between fractional CBCT and planned CT images was done to adjust setup error, and then the treatment began. CBCT images were acquired every 5 fractions until the end of treatment. Total 172 fractions' CBCT images were acquired, and one patient was excluded due to the error day for CBCT image acquisition.

Interfractional tumor

CBCT images acquired at the first fraction were transferred to the Pinnacle^3 planning systems to perform rigid registration with the planned CT. The GTV from the planned CT was copied to the first acquired CBCT images, and the GTV was adapted by the same experienced physician to obtain GTV_1. GTV_1 was then copied to CBCT images of later fractions (figure 1), and GTV_n was adapted on later fractional CBCT images. Fractional lymph nodes were maintained the same with planned CT (quality of CBCT images was not sufficient for an accurate assessment of the lymph nodes [12]).

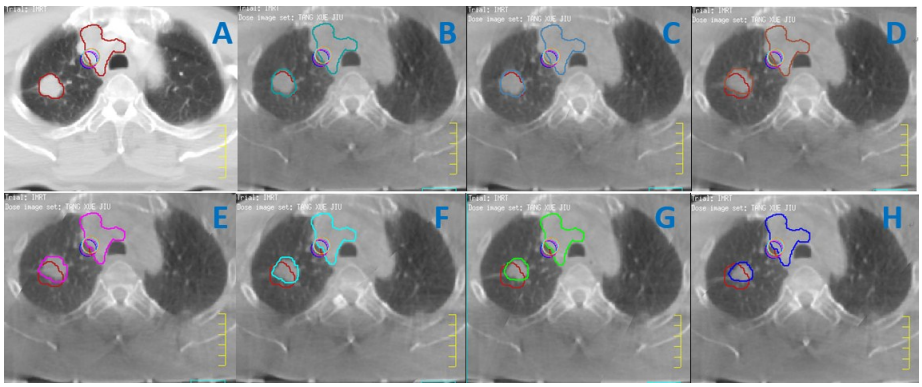

Figure 1. GTV contoured on planning CT **(A);** GTV_1 contoured on 1st CBCT scanning before 1st treatment **(B);** GTV_2 contoured on 2nd CBCT scanning before 6th treatment **(C);** GTV_3 contoured on 3rd CBCT scanning before 11th treatment **(D);** GTV_4 contoured on 4th CBCT scanning before 16th treatment **(E);** GTV_5 contoured on 5th CBCT scanning before 21th treatment **(F);** GTV_6 contoured on 6th CBCT scanning before 26th treatment **(G);** GTV_7 contoured on 7th CBCT scanning before 30th treatment **(H)**.

Tumor volume

Each patient's fractional GTV_n was copied to the planned CT, then the fractional GTV_n's volume was calculated. Grouping was performed by GTV initial volume (two groups: volume less than 100 cm^3, and greater than 100 cm^3), and each group's interfractional tumor changes was evaluated.

[DOI: 10.18869/acadpub.ijrr.18.3.467]

Tumor position:

7 points of interest（POI） were added on each patient's planned CT, then POI_n was automatically placed on the mass center of the related GTV_n, so the position of each GTV_n's center was obtained. GTV_1's center was used as a reference to separately evaluate the changes of the following GTV_n's center. Fractional 3D vector position changes were obtained by calculating the square root of the center's location values in three directions.

Tumor boundary

Every 2 fields with 0 and 90 degree were added separately for each GTV_n on the planned CT, and the field jaws fitted against the edge of the GTV_n. The locations of the jaws for all fields in the superior-inferior (SI), anterior-posterior (AP) and left-right (LR) directions were recorded separately, and then the borders of the fractional GTV_n in all directions can be obtained. GTV_1's borders were used as a reference to calculate borders changes of GTV_n in all directions.

Interfractional dose

When GTV_1 was copied on the planned CT images, PTV's margin was expanded on GTV_1 in all directions to form PTV_1. GTV_1 was removed from total lung to get the new total lung ($TLung_1$). The original plan was recalculated to get the PTV_1 and $TLung_1$ dose on planned CT. The above procedure was repeated for the following fractions, following PTV_n and $TLung_n$ doses were obtained. PTV_n and $TLung_n$ dose parameters were compared with the previous fraction. The formula was as follows: amount of fractional dose parameter increase (‰)= (current fraction's dose parameter - previous fraction's dose parameter) / previous fraction's dose parameter x 1000%.

Interfractional corrected dose

PTV_1 and $TLung_1$ were obtained by the above method. GTV_1's CT density was set as the mean density of the planned GTV; $TLung_1$'s CT density was set as the mean density of planned TLung. The original plan was recalculated to get the PTV_1 and $TLung_1$ dose distribution on planned CT. PTV_1 and $TLung_1$ dose parameters were recorded, then the above procedure were repeated for following PTV_n and $TLung_n$, their doses parameters were obtained. PTV_n and $TLung_n$ dose parameters were compared with the previous fraction. Workflow of the interfractional corrected dose calculation and comparison was presented (figure 2). The formula is as follows: fractional does parameter increase (‰) = (fractional dose parameter - the previous fraction's dose parameter) / the previous fraction's dose parameter × 1000%.

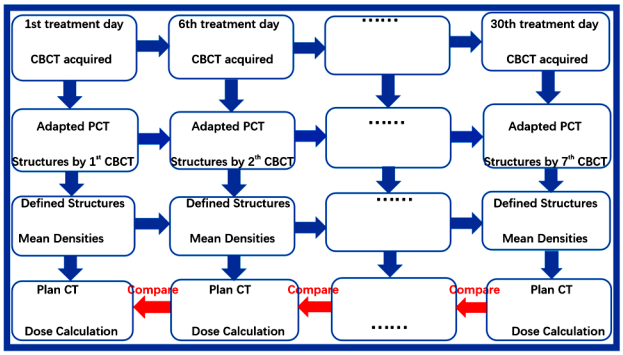

Figure 2. Workflow of the interfractional corrected dose calculation and comparison.

Statistical analysis

Paired t-test was used to compare every successive fraction's PTV and total lung dose parameters changes from the previous fraction by SPSS statistics V22.0 (IBM Corp., Armonk, NY). Differences were considered significant for $P < 0.05$. Quantitative data is expressed as mean value ± standard deviation (SD).

RESULTS

1. Initial GTV volume and fractional GTV_n volume change

The mean volume of all tumors for the first fraction was 115.54 cm^3 (58.05-381.75 cm^3). For the following fraction, the mean volumes of all tumors were 115.46 cm^3 (57.94-384.04 cm^3), 114.10 cm^3 (57.78-379.83 cm^3), 111.29 cm^3 (57.06-354.93 cm^3), 108.10 cm^3 (55.49-326.58 cm^3) and 105.45 cm^3 (53.96-311.85 cm^3),

[DOI: 10.18869/acadpub.ijrr.18.3.467]

respectively. 6 cases CBCT images were not acquired for the 7th fraction, so GTV_7 volume change was not evaluated (figure 3). In the group of cases whose initial GTV volume were greater than 100 cm^3, GTV_7 volume shrank 11.1% ($P<0.05$) on average when compared with GTV_1. In the group of cases whose initial GTV volume were less than 100 cm^3, GTV_7 volume shrank 9.8% ($P<0.05$) on average when compared with GTV_1.

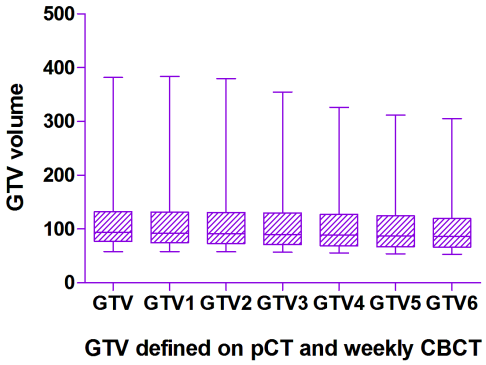

Figure 3. Statistical histogram of the first 6 fractions' GTV_n volume for 23 lung cancer cases.

2. Interfractional GTV_n mass centroid positions changes

The mass centroid positions in the LR direction changed for 14 cases, left and right lung cancer cases were respectively 3 cases and 11 cases (figure 4a). The centroid positions of left lung cancer moved towards right direction gradually through fractions, in the last CBCT scan, the maximum right offset of centroid position was 0.29 cm. The centroid positions of right lung cancer moved towards left direction gradually through fractions, in the last CBCT scan, the maximum left offset of centroid position was 0.59 cm.

The mass centroid positions in the AP direction changed for 13 cases, left and right lung cancer cases were respectively 4 cases and 9 cases (figure 4b); in these 13 cases, the centroid positions of 10 cases moved forward gradually through fractions，in the last CBCT scan, the maximum forward offset of centroid position was 0.29 cm. 2 of the other 3 cases had the centroid positions first moved backward, and then had a trend to move forward, one case had the centroid positions moved backward 0.4 mm at the 2nd and 3rd fractions compared to the 1st fraction, while at the 5th, 6th and 7th fraction, it had a forward shift of 0.5 mm; the other case had a backward shift of 0.5 mm at the 4th fraction, while at the 5th fraction, there was a 1 mm forward shift.

In the SI direction, since the quality of CBCT images was not sufficient for an accurate evaluation of lymph nodes shrinkage, the tumor lymph nodes on the first and last slices of the fractional CBCT images were not modified, so the mass centroid position offset analysis was not made in the SI direction.

3D vector mass centroid positions were observed for 19 cases (figure 4c). In the last CBCT scan, the maximum offset of 3D centroid position was 0.59 cm.

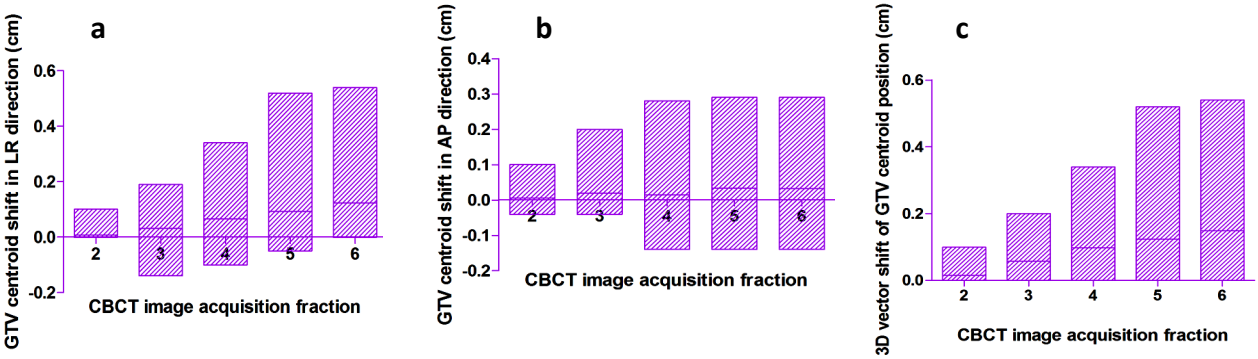

Figure 4. 14 cases centroid positions changes statistical histogram in the LR direction **(a);** 13 cases centroid positions changes statistical histogram in the AP direction **(b);** 19 cases centroid positions changes statistical histogram in 3D vector direction **(c)**.

[DOI: 10.18869/acadpub.ijrr.18.3.467]

3. Interfractional GTV_n border locations changes

11 cases were observed to have their tumors' back border shrunk forward in the AP direction, with maximum shrinkage of 0.6 cm.

GTV_n borders in the LR direction were observed for 15 cases. Among them 4 cases were left lung cancer (figure 5a) and a trend of rightward tumor borders shrinkage was observed. In the last CBCT scan, the maximum rightward shrinkage of the borders was 0.5 cm. The other 11 cases were right lung cancer (figure 5b), and a trend of leftward tumor borders shrinkage was observed for 10 cases. In the last CBCT scan, the maximum leftward shrinkage of the borders was 1.3 cm while the minimum was 0.4 cm. A rightward shrinkage trend was observed for the other case.

Interfractional PTV_n dose coverage changes

Through the CBCT image acquisition fractions, the dose coverage of fractional PTV_n V_{95}, V_{100} and V_{110} increased, while the amount of these parameters increase at each fraction compared to the previous was different. The similar results were seen whether CT images density correction was done or not (table 2). V_{95} and V_{100} of PTV_4 (i.e. the 16th treatment fraction) were observed largest dose coverage increase; V_{95}'s increase at this fraction was 1.41 ± 2.83‰) with no CT images density correction) and 1.00 ± 2.28‰) with CT images density correction); V_{100}'s increase was 3.26 ± 4.12‰) with no CT images density correction) and 2.14 ± 3.72‰) with CT images density correction).

CT images density correction seemly increased PTV_n V_{95} for first 5 times CBCT acquisition fractions (table 3). In the case of the 1st image acquisition fraction with CT images density correction, PTV_1 V_{95} increased 0.12 ± 0.28‰ ,P>4.468; PTV_2 V_{95} increased 0.10 ± 0.25‰ ,P>4.485. CT images density correction seemly also increased PTV_n V_{100}; but PTV_n V_{110} was seemly reduced, especially for the PTV_7.

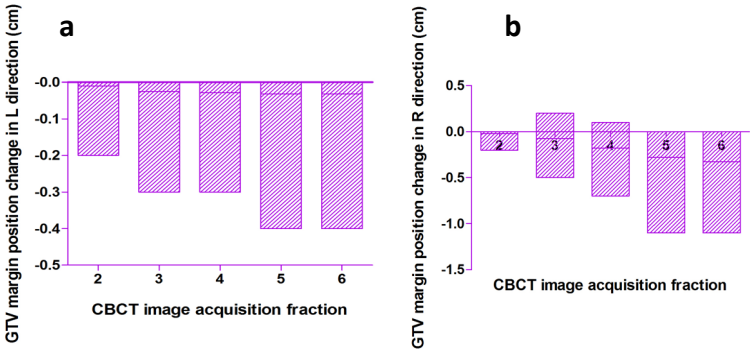

Figure 5. GTV_n borders rightward changes statistical histogram for 4 left lung cancer cases **(a)**; GTV_n borders leftward changes statistical histogram for 11 right lung cancer cases **(b)**.

Table 2. Increase of each PTV_n dose coverage from that of the previous.

	Mode	CBCT (2th)	CBCT (3th)	CBCT (4th)	CBCT (5st)	CBCT (6th)
ΔPTV V_{95}(‰)	Correction	0.82±1.33	1.24±1.94	1.41±2.83	0.97±1.78	0.47±0.88
	No correction	0.46±0.88	0.79±1.30	1.00±2.28	0.71±1.62	0.25±0.63
ΔPTV V_{100}(‰)	Correction	2.33±2.34	3.20±2.69	3.26±4.12	2.23±3.03	1.56±2.41
	No correction	1.41±1.49	1.70±4.06	2.14±3.72	1.42±2.83	1.00±1.98
ΔPTV V_{110}(‰)	Correction	7.10±5.10	13.82±13.48	7.82±13.77	4.56±16.63	-1.53±22.36
	No correction	1.96±31.39	-3.77±82.44	-2.93±65.00	29.00±129.07	3.09±28.82

Table 3. Impact of CT images density correction on PTV_n dose coverage.

	CBCT (1st)	CBCT (2nd)	CBCT (3rd)	CBCT (4th)	CBCT (5th)	CBCT (6th)	CBCT (7th)
PTV $(V_{95})_{cor}$-PTV $(V_{95})_{no\ cor}$	0.12±0.28	0.10±0.25	0.06±0.23	0.03±0.23	0.01±0.22	-0.02±0.21	-0.02±0.22
P	0.024	0.041	0.150	0.558	0.789	0.686	0.748
PTV$(V_{100})_{cor}$-PTV $(V_{100})_{no\ cor}$	0.16±0.88	0.12±0.85	0.02±0.60	0.14±0.60	0.12±0.56	0.25±0.64	0.10±0.41
P	0.339	0.468	0.861	0.362	0.396	0.098	0.374
PTV$(V_{110})_{cor}$-PTV $(V_{110})_{no\ cor}$	-0.34±0.83	-0.21±0.69	-0.24±0.79	-0.17±0.76	-0.41±0.88	-0.27±0.78	-0.35±0.72
P	0.101	0.271	0.220	0.388	0.219	0.141	0.044

[DOI: 10.18869/acadpub.ijrr.18.3.467]

Interfractional TLung$_n$ dose volume changes

Fractional TLung$_n$ V_5, V_{10}, V_{20} and V_{30} increased through the CBCT images acquisition fractions, and the increase of TLung$_n$ dose volume at each fraction compared to the previous was also different. The similar results were seen whether CT images density correction was done or not (table 4). TLung$_n$ dose parameters were observed the maximum increase at the 5th CBCT acquisition fraction (i.e., the 21st treatment fraction). The increases of TLung$_5$ V_5, V_{10}, V_{20} and V_{30} were 1.22±1.31‰, 1.93±2.32‰, 3.18±4.11‰ and 4.39±5.62‰ respectively (with no CT images density correction); the increases of TLung$_5$ V_5, V_{10}, V_{20} and V_{30} were 1.07±1.26‰, 1.81±2.38‰, 3.01±4.17‰ and 4.13±5.60‰ respectively (with CT images density correction).

Table 4. Increase of each TLung$_n$ dose volume from the previous.

	Mode	CBCT (2nd)	CBCT (3rd)	CBCT (4th)	CBCT (5st)	CBCT (6th)
Δlung V_5(‰)	No correction	0.54±0.42	0.94±1.05	1.09±1.23	1.22±1.31	1.05±1.23
	Correction	0.46±0.42	0.72±1.06	0.87±0.78	1.07±1.26	0.95±1.16
Δlung V_{10}(‰)	No correction	0.90±0.80	1.50±1.68	1.82±2.19	1.93±2.32	1.65±1.80
	Correction	0.85±0.78	1.33±1.73	1.66±1.69	1.81±2.38	1.58±1.81
Δlung V_{20}(‰)	No correction	1.38±1.25	2.46±2.92	2.97±3.89	3.18±4.11	2.70±3.06
	Correction	1.33±1.24	2.20±3.05	2.84±3.43	3.01±4.17	2.59±3.15
Δlung V30(‰)	No correction	1.87±1.69	3.29±3.94	4.04±5.27	4.39±5.62	3.66±4.22
	Correction	1.79±1.70	2.94±4.00	3.81±4.61	4.13±5.60	3.43±4.14

CT images density correction increased TLung$_n$ V_5 , V_{10} and seemly V_{20} (table 5), while decreased V_{30}.

Table 5. Impact of CT image density correction on TLungn dose volume.

	CBCT (1st)	CBCT (2nd)	CBCT (3rd)	CBCT (4th)	CBCT (5th)	CBCT (6th)	CBCT (7th)
Lung $(V_5)_{no\ cor}$-Lung $(V_5)_{cor}$	0.57±0.36	0.58±0.39	0.58±0.37	0.59±0.39	0.57±0.35	0.57±0.38	0.66±0.37
P	<0.001	<0.001	<0.001	<0.001	<0.001	<0.001	<0.001
Lung$(V_{10})_{no\ cor}$-Lung $(V_{10})_{cor}$	0.18±0.18	0.17±0.19	0.18±0.18	0.21±0.16	0.17±0.18	0.17±0.19	0.21±0.17
P	0.001	0.004	0.002	<0.001	0.003	0.002	0.001
Lung$(V_{20})_{no\ cor}$-Lung $(V_{20})_{cor}$	0.03±0.14	0.03±0.14	0.04±0.13	0.04±0.13	0.03±0.14	0.02±0.13	0.06±0.07
P	0.483	0.568	0.442	0.369	0.514	0.729	0.020
Lung$(V_{30})_{no\ cor}$-Lung $(V_{30})_{cor}$	-0.07±0.08	-0.07±0.08	-0.07±0.08	-0.07±0.08	-0.07±0.08	-0.08±0.08	-0.08±0.06
P	<0.001	0.002	0.001	0.004	0.002	0.001	0.001

DISCUSSION

Many studies [13-16] have reported the volume changes of tumor and its relationship with prognosis for stage I-III non-small cell lung cancer (NSCLC) radiotherapy, in order to identify markers associated with prognosis, provide optimal intervention time for NSCLC adaptive radiotherapy, improve the efficiency and effectiveness of adaptive radiotherapy for lung cancer, and save human resources.

As SCLC doubling time is short, it seemed that the patterns of tumor changes may be different from NSCLC, patterns of expansion and invasion to the periphery of SCLC have been rarely studied. There have been very few reports about the patterns of LD-SCLC patients' tumor changes through radiotherapy fractions, and the number of SCLC cases was really small in the few reports and their pathological stages were not centralized [7-8]. Definite patterns of tumor changes could be the precondition of robust adaptive radiotherapy for SCLC. Therefore, this study presented the patterns of tumor changes for LD-SCLC through radiotherapy fractions.

Various modality images can be used to monitor the changes of lung cancer tumor during radiotherapy [17,18]. CBCT guided IGRT has become a necessary step for radiotherapy, and CBCT has become a major method to evaluate the changes of lung cancer tumor [7-8].

Ellegaard *et al.* [7] reported that CBCT images acquired before each treatment could be used to accurately evaluate the tumor shrinkage for 37

[DOI: 10.18869/acadpub.ijrr.18.3.467]

SCLC cases, among which 15 cases showed shrinkage over 5 cm^3 or 15%. Knap *et al.* [8] also reported the use of CBCT before treatment to determine SCLC tumor volume changes through radiation therapy fractions. For all 6 SCLC cases, only 1 case showed tumor shrinkage over 15%. In our study, each CBCT images acquisition fraction's mean GTV volume reduced through fractions and the mean GTV_7 volume shrank about 10% compared to GTV_1.

Li *et al.* [19] reported that the tumor centroid means (±standard deviation) changes were 0.16 (±0.13) cm and 0.22 (±0.15) cm in LR and AP directions, respectively. Larger tumor centroid changes variations (≥5mm) were only observed in AP direction for one case. Sun *et al.* [20] reported that larger interfractional tumor centroid positions variations (≥5mm) were observed 57 fractions in total 153 lung cancer SBRT fractions, and we found the variations (≥5mm) occurred 3 fractions in LR direction in total 172 fractions for SCLC IMRT treatment. Our results were similar with Li's, and distinctly different from Sun's. Maybe the respiratory amplitudes of SBRT patients were larger and irregular in Sun's research, and our results may be related to the trend of interfractional tumor changes.

Li *et al.* [19] observed the means (±standard deviation) of tumor border location changes were 0.21 (±0.18) cm and 0.50 (±0.23) cm in LR and AP directions, and the mean border changes directions were toward to the centroid changes directions, which means the tumor shrank as expected. The results were consistent with what we have observed.

Increasing dose is one of the strategies to improve LD-SCLC patients' tumor local control rate and overall survival rate. However, the increase of radiation dose is restricted due to the need to spare OARs, which is a conclusion we can draw from reports about the failure to increase LD-NSCLC dose coverage [13]. Adaptive radiotherapy is a solution to increase LD-SCLC patients' overall radiation dose. It reduces radiation dose to normal tissues by intervening in time when tumor shrinks during radiotherapy. However, individual adaptive radiotherapy to patient means consuming time and human resources, while it is still not clear whether all patients can benefit from the same adaptive radiotherapy time.

P Berkovic, *et al.* [13] reported that LD-NSCLC patients who received sequential and concurrent chemoradiotherapy benefited the most from intervention at the 20^{th} and 15^{th} radiotherapy fractions respectively. In our study, the most increase of PTV_n dose coverage from the previous fraction was observed at 16^{th} treatment fraction, while the most increase of $TLung_n$ dose volume from the previous fraction was observed at 21^{th} treatment fraction. The results may provide a reference for potential timely intervention during the LD-SCLC radiotherapy.

As the impact of tumor volume changes on dosimetry is the concern of the study, so the results and conclusions were deducted by the assumption that the daily CBCT based IGRT treatment was collected, and daily CBCT was rigidly registered with plan CT, although CBCT images were actually collected every five fractions. The dose calculations were completed based on the planned CT images in this study, on which later fractional new structures volumes and their mean densities may be different from corresponding original structures. Thus the later fractional new structures' volumes on plan CT were adapted by corresponding fractional CBCT images while the structures mean densities were defined and remained same with corresponding original structures mean densities on plan CT images. In our study, samples needs to be accumulated continuously, and through various stratified analysis, combined with new technologies such as radiomics, we expect to have more reliable results, so as to provide more valuable information in order to realize individual chemoradiotherapy for LD-SCLC patients.

CONCLUSIONS

Tumor shrinkage seen through the radiotherapy fractions of limited disease small-cell lung cancer patients is closely related to the tumor's initial volume and location.

[DOI: 10.18869/acadpub.ijrr.18.3.467]

Target dose coverage and lung tissue dose volume increase while the tumor shrinks through fractions. It is appropriate for most patients to be intervened in the 21st radiotherapy fraction. CT image density correction slightly increases the target dose coverage (V_{95} and V_{100}) and lung tissue dose volume (V_5, V_{10} and V_{20}).

ACKNOWLEDGMENTS

This work was funded by Shen Kang Hospital Development Center (Grant No.16CR3056A).

Conflicts of interest*: *Declared none.

REFERENCES

1. P Goldstraw, J Crowley, K Chansky, LeslieSobin (2007) The IASLC Lung Cancer Staging Project: Proposals for the Revision of the TNM Stage Groupings in the Forthcoming (Seventh) Edition of the TNM Classification of Malignant Tumors. *Journal of Thoracic Oncology, **2(8)**:706-14*.
2. Lally BE1, Urbanic JJ, Blackstock AW, Miller AA, Perry MC (2007) Small Cell Lung Cancer: Have We Made Any Progress Over the Last 25 Years? *The Oncologist, **12**: 1096-1104*.
3. Aupérin, Anne Arriagada, Rodrigo Pignon, Jean-Pierre Le Péchoux, Cécile Gregor, and Joseph (1999) Prophylactic Cranial Irradiation for Patients with Small-Cell Lung Cancer in Complete Remission. *The New England Journal of Medicine, **341(7)**: 476-84*.
4. Takada M (2002) Phase III Study of Concurrent Versus Sequential Thoracic Radiotherapy in Combination With Cisplatin and Etoposide for Limited-Stage Small-Cell Lung Cancer: Results of the Japan Clinical Oncology Group Study 9104. *Journal of Clinical Oncology, **20(14)**: 3354-60*.
5. Han D, Qin Q, Hao SY, Huang W, Wei Y, Li BH (2014) Feasibility and efficacy of simultaneous integrated boost intensity-modulated radiation therapy in patients with limited-disease small cell lung cancer. Radiation Oncology, **9**: 280.
6. Liu ZY , Liu WH , Ji K, Wang P, Wang X, Zhao LJ (2015) Simultaneous integrated dose reduction intensity-modulated radiotherapy applied to an elective nodal area of limited-stage small-cell lung cancer. *Experimental and Therapeutic Medicine, **10**: 2083-87*.
7. Ellegaard MB, Knap MM, Hoffmann L (2013) Inter-tester reproducibility of tumor change in small cell lung cancer patients undergoing chemoradiotherapy. *Acta Oncologica, **52**: 1520-25*.
8. Knap MM, Hoffmann L, Nordsmark M (2010) Daily cone-beam computed tomography used to determine tumour shrinkage and localisation in lung cancer patients. *Acta Oncologica, **49**: 1077-84*.
9. Brade AM and Ian F (2006) Scheduling of Radiation and Chemotherapy for Limited-Stage Small-Cell Lung Cancer: Repopulation As a Cause of Treatment Failure? *Journal of clinical oncology, **24(7)**: 1020-21*.
10. Kazawa N, Kitaichi M, Hiraoka M, Togashi K, Mio N, Mishima M, Wada H (2006) Small cell lung carcinoma: Eight types of extension and spread on computed tomography. *Journal of Computer Assisted Tomography, **30(4)**: 653-661*.
11. Berkovic P, Paelinck L, Lievens Y, Gulyban A, Goddeeris B, Derie C, Surmont V, De Neve W, Vandecasteele K (2015) Adaptive radiotherapy for locally advanced non-small cell lung cancer, can we predict when and for whom? *Acta Oncologica, **54**: 1438-44*.
12. van Elmpt W, Ollers M, van Herwijnen H, den Holder L, Vercoulen L, Wouters M, Lambin P, De Ruysscher (2011) Volume or Position Changes of Primary Lung Tumor During (Chemo-) Radiotherapy Cannot Be Used as a Surrogate for Mediastinal Lymph Node Changes: The Case for Optimal Mediastinal Lymph Node Imaging During Radiotherapy. *Int J Radiat Oncol Biol phys, **79(1)**: 89-95*.
13. Mizuki N, Dahlberg SE, Fulton LE, Digumarthy SR, Hiroto H (2015) Volumetric tumor response and progression in EGFR-mutant NSCLC patients treated with erlotinib or gefitinib. *Acad Radiol, **23(3)**: 329–336*.
14. Jabbour SK, Kim S, Haider SA, Xu XT, Wu A (2015) Reduction in Tumor Volume by Cone Beam Computed Tomography Predicts Overall Survival in Non-Small Cell Lung Cancer Treated With Chemoradiation Therapy. *Int J Radiat Oncol Biol Phys, **92(3)**: 627–633*.
15. Hayes SA, Pietanza MC, O'Driscoll D, Zheng J, Moskowitz CS, Kris MG (2016) Comparison of CT volumetric measurement with RECIST response in patients with lung cancer. *Eur J Radiol, **85(3)**: 524–533*.
16. Zhang PP, Yorke E, Hu YC, Mageras G (2012) Predictive Treatment Management: Incorporating a Predictive Tumor Response Model Into Robust Prospective Treatment Planning for Non-Small Cell Lung Cancer. *Int J Radiat Oncol Biol Phys, **88(2)**: 446–452*.
17. Meng X, Frey K, Matuszak M, Paul S, Haken RT, Yu JM (2014) Changes in Functional Lung Regions During the Course of Radiation Therapy and Their Potential Impact on Lung Dosimetry for Non-Small Cell Lung Cancer. *Int J Radiat Oncol Biol Phys, **89(1)**: 145–151*.
18. Alexander SK, Tidwell VK, Engelbach JA, Alli VV, Nehorai A, Ming Y, Haris GV (2011) Quantitative Monitoring of Murine Lung Tumors by Magnetic Resonance Imaging. *Nat Protoc, **7(1)**: 10*.
19. Li Y, Ma Jl, Chen X, Tang FW, Zhang XZ(2016) 4DCT and CBCT based PTV margin in Stereotactic Body Radiotherapy (SBRT) of non-small cell lung tumor adhered to chest wall or diaphragm. *Radiation Oncology, **11**: 152*.
20. Sun Y, Lu Y, Cheng S, Guo W, Ye K, Zhao H, Zheng X, Ge H (2014) Interfractional Variations of Tumor Centroid Position and Tumor Regression during Stereotactic Body Radiotherapy for Lung Tumor. *Biomed Res Int, **2014**: 372738*.

[DOI: 10.18869/acadpub.ijrr.18.3.467]